European Journal of Pharmaceutics and Biopharmaceutics 144 (2019) 91–100

Contents lists available at ScienceDirect

European Journal of Pharmaceutics and Biopharmaceutics

journal homepage: www.elsevier.com/locate/ejpb

Bile salt-coating modulates the macrophage uptake of nanocores constituted by a zidovudine prodrug and enhances its nose-to-brain delivery

Alessandro Dalpiaz[a], Marco Fogagnolo[a], Luca Ferraro[b], Sarah Beggiato[b], Miriam Hanuskova[c], Eleonora Maretti[d], Francesca Sacchetti[d], Eliana Leo[d,*], Barbara Pavan[e,*]

[a] Department of Chemical and Pharmaceutical Sciences, University of Ferrara, Via Fossato di Mortara 19, I-44121 Ferrara, Italy
[b] Department of Life Sciences and Biotechnology, University of Ferrara and LTTA Center, Via L. Borsari 46, I-44121 Ferrara, Italy
[c] "Enzo Ferrari" Engineering Department, University of Modena and Reggio Emilia, Via Pietro Vivarelli 10, I-41125 Modena, Italy
[d] Department of Life Sciences, University of Modena and Reggio Emilia, Via Campi 103, I-41125 Modena, Italy
[e] Department of Biomedical and Specialist Surgical Sciences, University of Ferrara, Via L. Borsari 46, 44121 Ferrara, Italy

A R T I C L E I N F O

Keywords:
Nanoparticles
Bile acid salts
Macrophages
Uptake modulation
Nasal administration
Central nervous system

A B S T R A C T

We have previously demonstrated that the ester conjugation of zidovudine (AZT) with ursodeoxycholic acid (UDCA) allows to obtain a prodrug (U-AZT) which eludes the active efflux transporters (AET). This allows the prodrug to more efficiently permeates and remains in murine macrophages than the parent compound. Here we demonstrate that U-AZT can be formulated, by a nanoprecipitation method, as nanoparticle cores coated by bile acid salt (taurocholate or ursodeoxycholate) corona, without any other excipients. The U-AZT nanoparticles appeared spherical with a mean diameter of ~200 nm and a zeta potential of ~ −55 mV. During the incubation (5 h) in fetal bovine serum, the ursodeoxycholate-coated nanoparticle size did not change. Differently, taurocholate-coated particle size was firstly reduced and then increased up to 800 µm, thus suggesting the high aptitude of these nanoparticles to interact with serum proteins. The *in vitro* uptake of taurocholate coated particles by murine macrophages was strongly higher than that of ursodeoxycholate-coated particles or free U-AZT (~500% and ~7000%, respectively). AZT was also detected in macrophages following the prodrug uptake, with the greatest amounts observed after the taurocholate-coated nanoparticle incubation. As macrophages in the subarachnoid spaces of cerebrospinal fluid (CSF) constitute one of the most unreachable HIV sanctuaries in the body, we also tested the ability of taurocholate-coated nanoparticles (*i.e.*, nanoparticles highly internalized by macrophages) to reach them after their nasal administration in the presence or absence of chitosan. The results indicate that chitosan allowed to obtain a relatively high uptake (up to 4 µg/ml) of U-AZT in CSF. Taking into account that chitosan may promote the direct brain nanoparticle uptake, these findings can be considered an initial step toward the *in vivo* targeting of the subarachnoid macrophages by U-AZT prodrug.

1. Introduction

Zidovudine (AZT, Fig. 1) is a nucleoside/nucleotide reverse transcriptase inhibitor (NRTI) used, in combination with other antiretroviral agents, for highly active antiretroviral therapy (HAART) in advanced HIV-1 disease [1]. Although HAART is efficacious in reducing peripheral viral loads in HIV patients, a total eradication of the virus cannot be obtained. In fact, HIV-1 is also located in macrophages of central nervous system (CNS), known to harbor and replicate the virus and constituting one of the so-called "HIV sanctuaries" [2,3]. These are believed to be responsible for the rebound viraemia observed in nearly all people following treatment cessation [2,4]. A marked macrophage uptake of antiviral drugs or prodrugs, not only at the peripheral level but also in the "HIV sanctuaries" mainly located in the subarachnoid spaces of cerebrospinal fluid (CSF), is therefore required for the eradication of HIV. Unfortunately, the antiretroviral drugs are unable to reach therapeutic concentrations in the CNS [5], being substrates of active efflux transporters (AET) expressed on the membranes of lymphocytes [6–8], macrophages [9] and the cells that constitute the blood–brain (BBB) and blood-cerebrospinal fluid (BCSFB) barriers [10–12]. In particular, it is currently known that AZT is not a glycoprotein P (P-gp) substrate [13] and that breast cancer resistance protein

* Corresponding authors.
E-mail addresses: dla@unife.it (A. Dalpiaz), marco.fogagnolo@unife.it (M. Fogagnolo), frl@unife.it (L. Ferraro), sarah.beggiato@unife.it (S. Beggiato), miriam.hanuskova@unimore.it (M. Hanuskova), eleonora.maretti@unimore.it (E. Maretti), francesca.sacchetti@unimore.it (F. Sacchetti), leoeli27@unimore.it (E. Leo), pvnbbr@unife.it (B. Pavan).

https://doi.org/10.1016/j.ejpb.2019.09.008
Received 15 January 2019; Received in revised form 26 August 2019; Accepted 8 September 2019
Available online 12 September 2019
0939-6411/

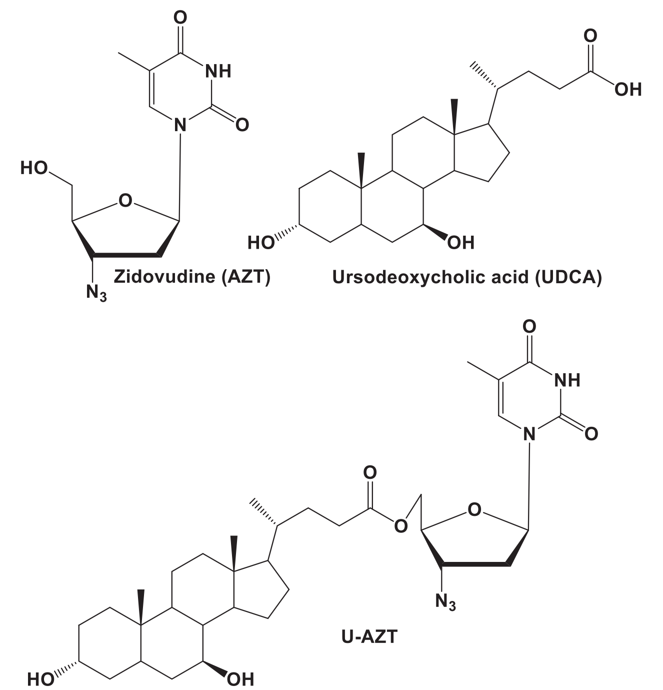

Fig. 1. Chemical structures of zidovudine (AZT), ursodeoxycholic acid (UDCA) and the prodrug (U-AZT) obtained by AZT/UDCA ester conjugation.

(bcrp) transporters are not active in limiting its CNS distribution [14]. On the other hand, organic anion transporter (Oat) systems have been suggested to be involved in the AZT efflux by choroid plexus [15], whereas the activity of multidrug resistance protein (MRP) 4 or MRP5 was proposed to induce the AZT efflux from macrophages [9].

Thus, there is a strong need of new strategies to improve the delivery of antiretroviral drugs in the CNS as well as their uptake by CNS macrophages. Moving from this concept, we have recently demonstrated that AZT, can be conjugated with the ursodeoxycholic acid (UDCA, Fig. 1) in order to obtain a prodrug (U-AZT, Fig. 1) able to elude, without inhibiting, the AET systems [16] and, therefore, to permeate and remain in murine macrophages with a twenty times higher efficiency than AZT [17].

Based on the promising results we obtained, the aim of the present study was to further improve the U-AZT uptake in macrophages that harbor HIV and constitute the only site of the virus replication in the brain [18,19]. It is known that the use of nanoparticulate systems appears a promising strategy to potentiate the therapeutic effects of drugs that, upon the administration as free form, difficultly reach their target sites in the body [20,21].Taking into account these aspects, we developed innovative nanoparticles constituted by self-assembled cores of U-AZT coated with bile salt (taurocholate or ursodeoxycholate) coronas. These nanoparticles have been characterized *in vitro* for their size, zeta potential, particle distribution, stability in serum, U-AZT content, toxicity and the ability to improve U-AZT uptake by macrophages.

Finally, in view of the encouraging *in vitro* results we obtained, we also performed *in vivo* experiments to possibly individuate a strategy to improve the brain targeting of the U-AZT after the intranasal administration of developed nanoparticles to rats. To this aim, we selected the nanoparticles showing a high capability to be internalized into macrophages to prepare their water suspensions in the absence or in the presence of chitosan hydrochloride. Chitosan has been chosen considering its ability to transiently open the tight junctions of nasal mucosa [22] and its potential aptitude in inducing nanoparticles to cross intranasal epithelium by a paracellular pathway [23] in order to verify the opportunity to further enhance the CSF U-AZT levels and, consequently, the prodrug uptake by CNS macrophages.

2. Materials and methods

2.1. Materials

Ursodeoxycholic acid (UDCA) was kindly supplied by ICE Srl (RE, Italy) and used without purification. AZT was purchased from Carbosynth Limited (Berkshire, UK). U-AZT was synthesized according to published procedure [16]. Sodium ursodeoxycholate was obtained by stoichiometric neutralization of UDCA by a sodium hydroxide solution. 7-n-Propylxanthine (7-n-PX), bovine serum albumin (BSA) and sodium taurocholate were obtained from Sigma Aldrich (St. Louis, MO, USA). Methanol, acetonitrile, ethyl acetate and water (Sigma Aldrich) were of high performance liquid chromatography (HPLC) grade. Chitosan hydrochloride (Protasan UP CL 113) was purchased from FMC BioPolymer AS (Drammen, Norway). The reversed-phase column (Hypersil BDS C-18 5U cartridge column, 150 mm × 4.6 mm i.d.) and the guard column (packed with Hypersil C-18 material) were obtained from Alltech Italia Srl BV (Milan, Italy). All other reagents and solvents were of analytical grade (Sigma-Aldrich). The murine macrophage cell line J774A.1 was obtained from the American Type Culture Collection (LGC Standards, Milan, Italy). Dulbecco's modified Eagle's medium + Glutamax, fetal bovine serum (FBS), penicillin, and streptomycin were provided by Invitrogen (Life Technologies, Milan, Italy).

2.2. In vitro experiments

2.2.1. Preparation of sodium taurocholate or sodium ursodeoxycolate nanoparticles

Sodium taurocholate or sodium ursodeoxycolate coated U-AZT nanoparticles (nano-tauro and nano-UDCA, respectively) were obtained by using the nanoprecipitation method with slight modifications [24]. Briefly, a solution of U-AZT in methanol (MeOH; 0.5% w/v) was dropwise-added into an aqueous solution of sodium taurocholate (nano-tauro) or sodium ursodeoxycolate (nano-UDCA) (0.025% w/v) as surfactant kept at 25 °C under gentle stirring (IKA Labortechnik, Staufen im Breisgau, Germany). The resulting nanosuspensions were maintained under gentle mechanical mixing overnight to evaporate the organic solvent. After solvent evaporation, the nanoparticles were freeze-dried at –55 °C at a pressure of 10^{-4} Torr for 36 h (Lyovac GT2, Leybold-Heraues GmbH, Koln, Germany) and stored as dry powder at 25 °C.

2.2.2. Nano-tauro and nano-UDCA characterization

Nanosuspensions were characterized for size, zeta potential, and particle distribution by photon correlation spectroscopy (PCS) (Zetasizer, Malvern Instrument, UK) either before or after the freeze-drying process. Before freeze-drying, the samples were diluted (1:10) in deionized water to avoid multi-scattering events, while freeze-dried samples were re-suspended in deionized water (0.1 mg/ml). The suspensions were then examined to determine size (Z-Average), zeta potential and polydispersity index (PDI). The reported data represent the mean of three independent experiments.

Nanoparticle morphology was analysed by field-emission gun scanning electron microscopy (SEM-FEG, Nova 11 NanoSEM 450, Fei, Eindhoven, The Netherlands) using both the scanning electron microscopic (SEM) mode and the scanning transmission electron microscopic (STEM) mode. For the SEM mode, few drops of the freshly prepared nanoparticle suspensions (nano-tauro and nano-UDCA) diluted in deionized water; (1:10) were placed on an aluminum stub (TAAB Laboratories Equipment Ltd, Aldermaston, Berks, UK) previously covered with a double sided sticky tab (TAAB Laboratories Equipment Ltd, Aldermaston, Berks, UK). After drying, the stubs were vacuum coated with gold–palladium in an argon atmosphere for 60 s (Sputter Coater Emitech K550, Emitech LTD, Ashford, Kent, UK).

For the TEM mode, a STEM detector characterised by a low voltage electron beam (30 kV) was employed. TEM 200 mesh Formvar/Carbor coppergrids (TAAB Laboratories Equipment Ltd, Berks UK) were immersed in the diluted (1:10 v/v in water) freshly prepared nanosuspensions and dried under normal room conditions (25 °C, 760 mmHg) before the analysis.

2.2.3. Measurement of nano-tauro and nano-UDCA U-AZT content

To determine the content of U-AZT in the powders, the nanoparticles (~2 mg) were weighted using a high precision analytical balance (d = 0.01 mg; Sartorius, model CP 225D, Goettingen, Germany) and dissolved in MeOH (0.38 mg/mL); thereafter the samples were diluted 1:2 with water and filtered aliquots of these solutions (0.45 μm) were injected into a HPLC system for U-AZT assay. The percent drug loading in nanoparticle was calculated according to the following equation:

$$Drug\ loading\ \left(\%\frac{W}{W}\right) = \frac{mass\ of\ drug\ in\ nanoparticles}{mass\ of\ nanoparticles} \times 100 \tag{1}$$

All the reported values represent the mean of three independent experiments.

2.2.4. Nanoparticle stability in serum

In order to evaluate the stability of the nanoparticles in serum, 10 mg of liophilized nano-tauro and nano-UDCA were added to 1 mL of fetal bovine serum (FBS) solution (100% FBS; 37 °C) [25]. At selected time points, ranging from 15 min to 5 h, aliquots of the suspensions were diluted with MilliQ water (1/10 v/v) and size, PDI and zeta potential were measured by the DLS analysis (Malvern Z-Sizer, Zetasizer version 6.12, Malvern Instruments, Worcs, U.K). Each measurement was performed in triplicate.

2.2.5. U − AZT and AZT HPLC analysis

U − AZT prodrug and its hydrolysis product (AZT) levels were quantified by HPLC. The chromatographic apparatus consisted of a modular system (model LC-10 AD VD pump and model SPD-10A VP variable wavelength UV–vis detector; Shimadzu, Kyoto, Japan) and an injection valve (20 μL sample loop; model 7725; Rheodyne, IDEX, Torrance, CA, USA). The detector was set at 260 nm. Peak separations were performed at room temperature on a 5 μm Hypersil BDS C-18 column (150 mm × 4.6 mm i.d.; Alltech Italia Srl, Milan, Italy), equipped with a guard column packed with the same Hypersil material. Data acquisition and processing were accomplished by using the CLASS-VP Software, version 7.2.1 (Shimadzu Italia, Milan, Italy). A gradient elution program using a mixture of water and MeOH as mobile phase was used. The program was as follow (flow rate = 1 mL/min): isocratic elution with 20% (v/v) MeOH in water for 10 min; 1 min linear gradient to 75% (v/v) MeOH in water; elution with this mobile phase composition for 10 min. After each cycle, the column was conditioned with 20% (v/v) MeOH in water for 10 min. The retention times for AZT and the U − AZT prodrug were 6.5 and 19.6 min, respectively. The HPLC assay of U − AZT alone was performed isocratically with 80% (v/v) MeOH in water. In this case, the retention time of U − AZT was 4.8 min. The analysis precision was evaluated by repeating (n = 6) the measurement of the same sample solution of 50 μM AZT (13.4 μg/mL) or U-AZT (32.1 μg/mL) dissolved in MeOH; under these conditions, the observed relative standard deviation (RSD) values for AZT and U-AZT were 0.91% and 0.94%, respectively. Calibration curves of peak areas *versus* concentration were linear (n = 8, r ≥ 0.997, $P < 0.0001$) in the range of 0.5–100 μM for AZT (0.13–26.7 μg/mL) and U − AZT (0.32–64.18 μg/mL). For CSF simulation, standard aliquots of balanced solution (PBS Dulbecco's without calcium and magnesium) in the presence of 0.45 mg/mL BSA were used [26,27]. In this case, the chromatographic precision was evaluated by repeated analysis (n = 6) of the same sample solution containing 2.0 μM AZT (0.53 μg/mL) or U − AZT (1.28 μg/mL) and was represented by RSD values of 0.94% and 0.96%, respectively. The calibration curves of peak areas *versus* concentration were linear (n = 8, r ≥ 0.992, $P < 0.0001$) over the range of 0.5–20 μM for AZT (0.135 – 5.32 μg/mL) and U-AZT (0.320 – 12.84 μg/mL).

2.2.6. Cell culture and uptake of U-AZT in macrophages

Adherent cultured J774A.1 macrophages were grown in Dulbecco's modified Eagle's medium + Glutamax supplemented with 10% FBS, 100 U/mL penicillin and 100 μg/mL streptomycin (37 °C; humidified atmosphere of 95% O_2 with 5% of CO_2). Subcultures were prepared by scraping, whereby cells were re-suspended in the medium, aspirated and dispensed into new flasks. For the U-AZT cell uptake studies, J774A.1 cells were seeded in 12-well culture plates (1 mL/well; 5×10^5 cells). When semi confluent monolayer was formed, the cells were subsequently exposed to (*i*) 1 mL of 100 μM U-AZT (64.18 μg/mL) solution in growth medium for 15 min, in the absence or in the presence of 0.32 mg/mL of sodium taurocholate or 0.32 mg/mL sodium ursodeoxycholate, and (*ii*) 1 mL of U-AZT nanoparticle suspensions in growth medium in the presence of sodium taurocholate (nano-tauro) or sodium ursodeoxycholate (nano-UDCA); the amount of the suspended nanoparticles in growth medium was equivalent to 100 μM U-AZT (64.18 μg/mL). At the end of the treatment, the incubation medium was removed, cells were washed twice with the incubation medium and then twice with PBS. At this point, pairs of culture plates, treated as previously described, were split out in order to obtain the lysis of the cells or to perform their counting. The macrophages were lysed by adding pure water (0.3 mL per well) and freezing them in the presence of water (−80 °C; 60 min). This procedure ensured the best osmotic shock and cell membrane breaking [28,29], as evidenced by microscopic observation, allowing to completely deliver the intracellular content after thawing and scraping of lysed macrophages. Finally, cell lysates were transferred to glass tubes, dried under nitrogen stream, resuspended in 0.2 mL of MeOH and centrifuged (5 min at 13,000 × *g*) to remove cell debris. The supernatant (10 μL) was used to measure the levels of the test substrates by HPLC analysis. A third set of control 12-well culture plates was treated as described above but in the absence of cells, in order to evaluate the amounts of U-AZT adsorbed in the wells. These amounts have been subtracted from the U-AZT levels measured in the presence of macrophages under the corresponding conditions. J774A.1 cells were counted by using the Scepter 2.0 cell counter (Merck Millipore, Milan, Italy). Briefly, the cells were scraped and re-suspended in the culture medium; thereafter, the resultant cell suspensions were transferred to 1.5 mL microcentrifuge tubes and the cells were counted with the counter equipped with a 60 μm sensor tip, according to the manufacturer's recommendation. The volume of the macrophages measured by the cell counter was 1.7 ± 0.1 pL.

All the reported J774A.1 cell results represent the mean of four independent experiments.

2.2.7. Toxicity evaluation (MTT assay)

J774A.1 cells were seeded in 96-well plates at a density of 8,000 cells per well and reached an optimal population density within 48–72 h. The cells were then incubated for 15 min in 200 μL of culture medium in the presence or in the absence of 100 μM U-AZT (free prodrug or nanoparticulate formulations). The U-AZT free form was incubated in the absence or in the presence of 0.32 mg/ml of sodium taurocholate or sodium ursodeoxycholate. After this period, the incubation medium was removed and replaced with 200 μL of fresh culture medium, and 20 μL of 3-(4,5-dimethylthiazol-2-yl)-2,5-diphenyltetrazolium bromide (MTT) stock solution (5 mg/mL) were added to each well (37 °C; 4 h). A negative control of 20 μL of the MTT stock solution added to 200 μL of medium alone was included. Then, 100 μL of DMSO were added to each well and maintained for 2 h (37 °C in an orbital shaker incubator). Finally, the absorbance of each well was measured at 570 nm using a microtiter plate reader (Sunrise® Microplate Reader, Tecan Trading AG, Switzerland). The values were expressed as cell vitality percentages with respect to control. Each reported value represents the mean of four independent incubation experiments.

2.3. *In vivo experiments*

2.3.1. *Nasal administration of nano-tauro U−AZT*

Nasal administration of nano-tauro U−AZT was performed on anesthetized male Wistar rats (Charles River, Lecco, Italy) laid on their backs, by introducing, into each rat nostril, 55 µL of an aqueous nanoparticle suspension (12 mg/mL) in the absence or in the presence of chitosan hydrochloride (6 mg/mL), used as absorption enhancer [30]. After the nanoparticle administration, CSF samples (50 µL) were collected at fixed time points, by cysternal puncture method, as previously described [31,32]. A total volume of about a maximum of 150 µL of CSF/rat (*i.e.*, three 50 µL samples/rat) was collected during the experimental session, choosing the time points (n = 4–5) in order to allow the restoring of the CSF physiological volume. CSF samples (10 µL) were immediately injected into the HPLC system for AZT and U−AZT level detection. Each time-point value represents the mean of at least four experiments. No more than three CSF samples/rat have been obtained. The areas under the concentration curves of U–AZT in the CSF (AUC, µg mL^{-1} min) were calculated using the trapezoidal method, by using the computer program GraphPad Prism (GraphPad, San Diego, CA).

All *in vivo* experiments were performed in accordance with the European Communities Council Directive of September 2010 (2010/63/EU), the Declaration of Helsinki, and the Guide for the Care and Use of Laboratory Animals as adopted and promulgated by the National Institutes of Health (Bethesda, Maryland). The protocol of all the *in vivo* experiments was approved by the Italian Ministry of Health. Every effort was made to reduce the number of animals and their suffering.

2.4. *Statistical analysis*

Student's *t* test or by one-way ANOVA, followed by Bonferroni posttest were used, as appropriate, for the statistical evaluation of the results (GraphPad Prism; GraphPad, San Diego, CA). P values < 0.05 were considered to be statistically significant.

3. Results

3.1. *In vitro experiments*

3.1.1. *Preparation and characterization of nano-tauro and nano-UDCA*

Nano-tauro and nano-UDCA were prepared using a nanoprecipitation method. The poorly water-soluble U-AZT constituted the hydrophobic core of nanoparticles, while the sodium salt of bile acids served as surfactant. The size, PDI and zeta potential of freshly prepared (FP) nanoparticles are shown in Table 1. The mean diameters of nano-tauro and nano-UDCA were 190 and 215 nm, respectively. Moreover, a low PDI value was observed in both formulations, thus suggesting a narrow size distribution. The zeta potentials of nano-tauro and nano-UDCA were strongly negative (−55.6 and −51.8 mV, respectively), probably due to the presence of bile salts on the particle surface.

The nanoparticle suspension was lyophilized and the freeze-dried power was re-dispersed in deionized water at the same concentration as in the fresh preparation; the size and the zeta potential of the reconstituted nanoparticles (reconstituted lyophilized powder; RLP) are also indicated in Table 1. There were no significant size, zeta potential and PDI value differences between the freshly prepared and RLP nanoparticles, thus indicating the ability of nano-tauro and nano-UDCA powders to be re-constituted after lyophilization. The U-AZT loading in the RLP was 16.67% w/w and no differences were observed between the two formulations.

Table 1
Size, polydispersity index (PDI) and zeta potential of freshly prepared (FP) and reconstituted (RLP) nanoparticles.

Nanoparticle	Z-average (nm)	PDI	Zeta potential (mV)
Nano-tauro FP	190 ± 10	0.063 ± 0.02	−55.6 ± 6.53
Nano-tauro- RLP	217 ± 15	0.066 ± 0.03	−59.6 ± 9.11
Nano-UDCA FP	215 ± 20	0.116 ± 0.07	−51.8 ± 7.46
Nano-UDCA RLP	248 ± 20	0.183 ± 0.09	−61.4 ± 6.91

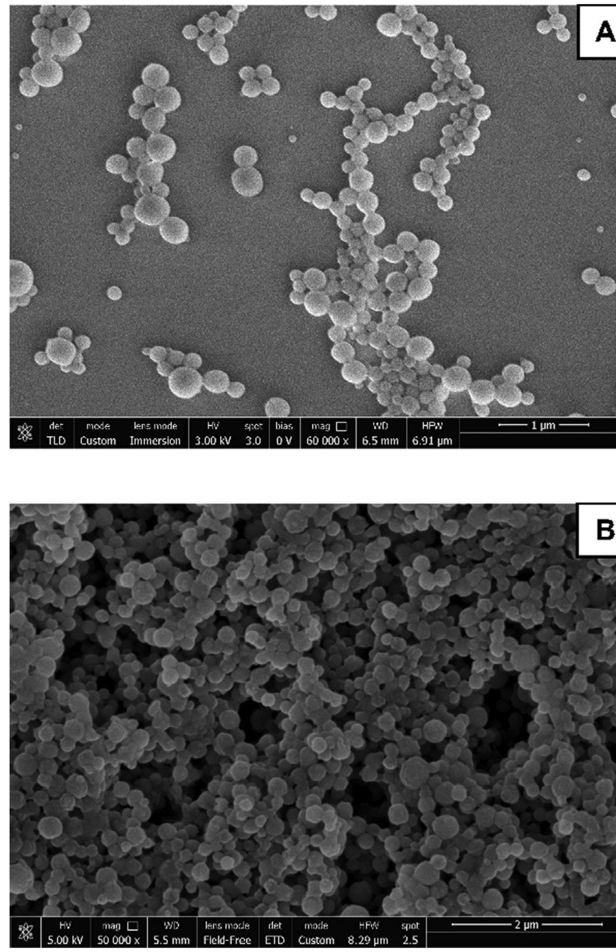

Fig. 2. SEM microphotographs of nano-UDCA (A) and nano-tauro (B).

Morphological studies were performed by SEM-FEG instrument, using the SEM modality to observe the nanoparticles in solid form, and STEM modality to visualize the nanoparticles in suspension.

Fig. 2 shows exemplificative SEM microphotographs of nano-UDCA (A) and nano-tauro (B). The morphological analysis (Fig. 2(A and B)) indicated the presence of spherical nanoparticles in the U-AZT/bile acid sodium salt nanocomposites, showing distinct particles with a smooth surface and sizes consistent with PCS analysis (Table 1).

Using the STEM modality (Fig. 3(A and B)), it has been possible to demonstrated that the nanosuspensions appeared to be formed by dark spherical particles surrounded by a weak-contrast region, possibly attributable to a multilayer bile acid salt-corona.

In order to demonstrate that the observed weak-contrast region represented the multilayer bile acid salt-corona, freshly prepared nano-UDCA were purified for 24 h by dialysis (Dialysis Tubing - Visking MWCO-12-14000 Daltons, Medicell International Ltd, London) and, then analysed by STEM (Fig. 3C). Under these experimental conditions, there was no visible corona around the particles, thus confirming the presence of the bile acid salt multilayers in not-purified nanoparticles.

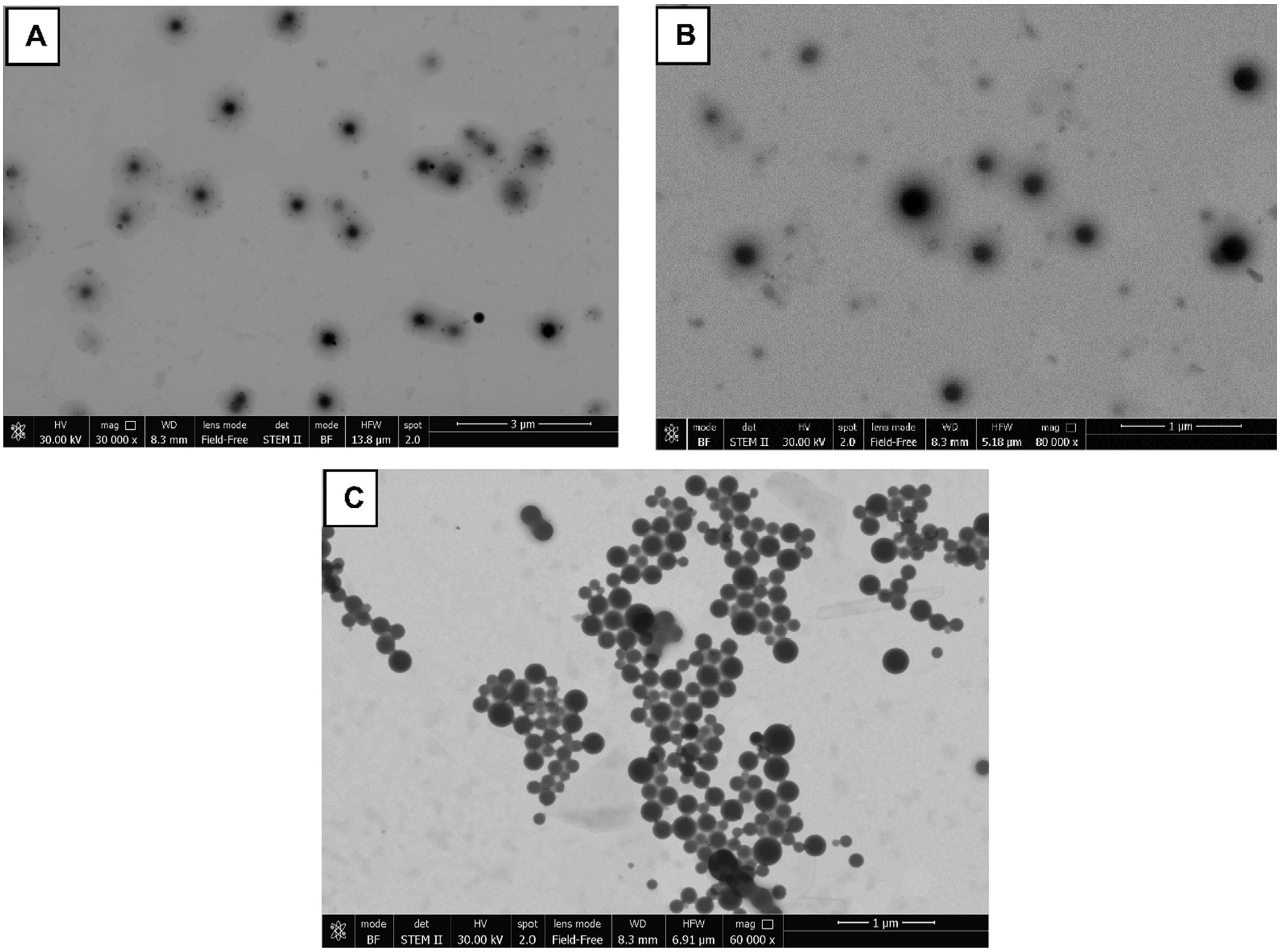

Fig. 3. Representative STEM images of nano-UDCA (A), nano-tauro (B) and (C) nano-UDCA after purification by dialysis.

3.1.2. Nanoparticle stability in serum

Both FP or RLP nanoparticles were perfectly stable in an aqueous suspension for at least 24 h at room temperature. Under these conditions, nanoparticle sizes remained within the error range reported in Table 1. To test the possible effect of the serum proteins on the particle in suspensions, the *in vitro* dimensional stability of nano-tauro and nano-UDCA FBS suspensions was evaluated by measuring particle size, PDI and zeta potential at different time-points (up to 5 h from the particle suspension).

For both the formulations, the PDI value increased during the considered time period until values ranging between 0.4 and 0.5, according the feature of free FBS solution. Moreover, a reduction of the zeta potential value for both the nanoparticles was observed (values ranging between −25 and −35 mV) probably due to the shield effect of the serum proteins.

Regarding the particle size (Fig. 4), the nano-tauro underwent to a drastic reduction of the average size (from 200 to 50 nm) in the first few min after their suspension; afterward, a slow and progressive size increase occurred, reaching a value of ~800 nm after 5 h of incubation. These data suggest the existence of strong interactions between these nanoparticles and the serum components. On the other hand, no significant ($P > 0.05$) nano-UDCA size changes were detected during the experimental period, clearly indicating the existence of very weak interactions between these nanoparticles and serum proteins.

3.1.3. U-AZT macrophages uptake

The incubation of free U-AZT (100 μM; 15 min) with macrophages led to detect 238 ± 25 ng (*i.e.*, 0.37 ± 0.04 nmoles) of this prodrug in 10^6 cells, as reported in Fig. 5A. Free U-AZT macrophages uptake was not significantly influenced ($P > 0.05$) when the prodrug incubation was performed in the presence of sodium taurocholate (263 ± 36 ng; 0.41 ± 0.06n moles in 10^6 cells) or sodium ursodeoxycholate (441 ± 51 ng; 0.69 ± 0.08n moles in 10^6 cells), the surfactants used for the nanoparticle formulations (Fig. 5A). On the other hand, the incubation of the same amounts of U-AZT and surfactants, formulated as nano-tauro or nano-UDCA, significantly improved the uptake of U-AZT in macrophages. In particular (Fig. 5A), following the incubation of the nano-tauro with macrophages we measured 16321 ± 2458 ng

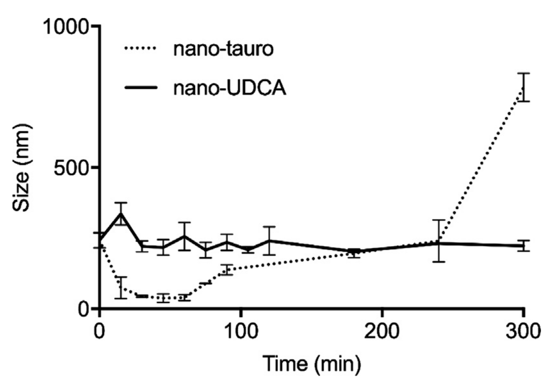

Fig. 4. Size profiles of nano-tauro and nano-UDCA particles during their incubation in fetal bovine serum. The data are reported as the mean ± SEM of three independent experiments.

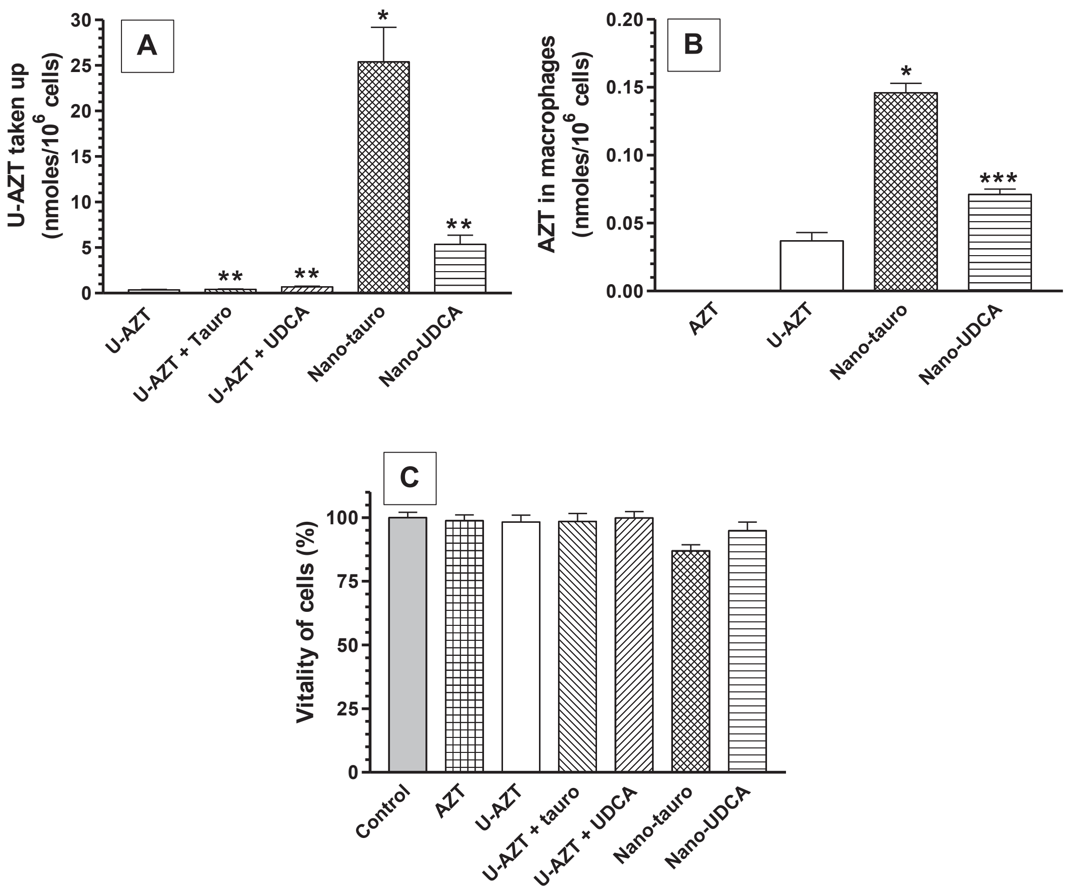

Fig. 5. Intracellular levels of U–AZT **[A]** or AZT **[B]** and percentage of cell vitality with respect to control **[C]** following 15 min of incubation with J774A.1 murine macrophages as 100 μM free solution (U-AZT or AZT) in the absence or in the presence of free taurocholate (U-AZT + Tauro) or free ursodeoxycholate (U-AZT + UDCA) and as nanoparticulate formulations obtained in the presence of taurocholate (Nano-tauro) or urspdeoxycholate (Nano-UDCA). The amount of nanoparticles incubated was equivalent to 100 μM U-AZT. The data are reported as the mean ± SEM of four independent experiments. *: P < 0.001 *versus* U-AZT and *versus* Nano-UDCA; **: P > 0.05 *versus* U-AZT; ***: P < 0.01 *versus* U-AZT.

(25.4 ± 3.8 n moles) of U-AZT in 10^6 cells, an amount ~70 times higher than that obtained with the free prodrug (P < 0.001). The incubation of the nano-UDCA particles allowed us to obtain an uptake of U-AZT corresponding to 3448 ± 637 ng (5.37 ± 0.99n moles) in 10^6 cells. This amount was ~14 times higher than that obtained with the free prodrug, but this difference was not statistically significant (P > 0.05). Compared to nano-tauro, nano-UDCA particles led to a five-times lower U-AZT macrophage uptake, a difference considered significant by the statistical analysis (P < 0.001).

3.1.4. AZT macrophages uptake

Fig. 5B shows that AZT was not detected within the macrophages after a 15 min incubation period of the compound (100 μM). On the contrary, the incubation (15 min) of U-AZT allowed us to detect 9.9 ± 1.8 ng (0.037 ± 0.007 nmoles) of AZT in 10^6 cells, and this value was significantly increased when U-AZT (100 μM) was incubated as nano-UDCA (18.9 ± 1.0 ng; 0.071 ± 0.004 nmoles of AZT in 10^6 cells; P < 0.01) or nano-tauro (39.0 ± 1.8 ng; 0.146 ± 0.007 nmoles of AZT in 10^6 cells; P < 0.001).

3.1.5. Toxicity evaluation

As reported in Fig. 5C, the incubation of macrophages with AZT, U-AZT, U-AZT in the presence of sodium taurocholate or sodium ursodeoxycholate, nano-tauro or nano-UDCA did not induce significant toxicity effects on the cells, thus indicating the biocompatibility of the tested nanoparticles and their free components. Similar results were also obtained after 30 and 60 min of incubation (*data not shown*).

3.2. In vivo experiments

3.2.1. Nasal nano-tauro administration

The nano-tauro were nasally administered as water suspension in the presence or absence of chitosan hydrochloride (6 mg/mL). In particular, the rats received ~200 μg of U-AZT by administration of 55 μL of suspension to each nostril. As reported in Fig. 6, the nasal nano-tauro administration produced detectable amounts of U-AZT in the CSF of

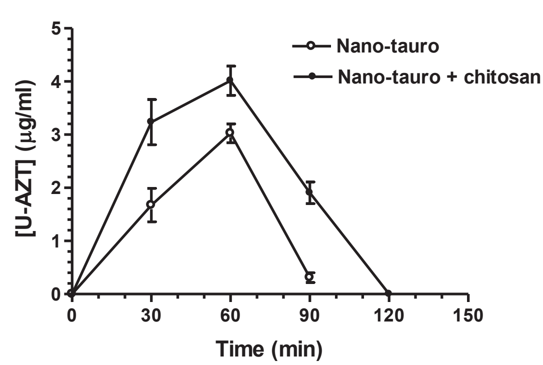

Fig. 6. U − AZT concentrations (μg/mL) detected in the CSF after nasal administration of a water suspension nano-tauro particles in the absence (nano-tauro) or in the presence (nano-tauro + chitosan) of chitosan hydrochloride (6 mg/mL). Each dose contained 200 μg of U − AZT. Data are expressed as the mean ± SEM of four independent experiments.

rats. In particular, in the absence of chitosan, nano-tauro suspension administration led to detect 1.68 ± 0.31 μg/mL and 3.03 ± 0.18 μg/mL of the prodrug 30 and 60 min after administration, respectively; U-AZT appeared almost completely eliminated from the CSF of rats 90 min after the administration, showing a concentration value below the calibration curve (0.31 ± 0.09 μg/mL) at this time-point. Interestingly, in the presence of chitosan, nano-tauro suspension (nano-tauro + chitosan) allowed us to detect 3.23 ± 0.43 μg/mL, 4.02 ± 0.28 μg/mL and 1.91 ± 0.21 μg/mL of the prodrug 30, 60 and 90 min after administration, respectively; 120 min after the nano-tauro + chitosan administration, U-AZT appeared completely eliminated from the rat CSF.

The area under concentration curve (AUC) values obtained for U−AZT in the CSF, following the nasal administration of the nano-tauro suspension in the absence of chitosan, was 145.7 ± 7.8 $\mu g \cdot mL^{-1} \cdot min$. This value was significantly lower ($P < 0.0001$) than that obtained following the nasal administration of nano-tauro + chitosan (274.7 ± 11.6 $\mu g \cdot mL^{-1} \cdot min$), thus indicating the ability of chitosan to double up the uptake of U-AZT in the CSF when the prodrug is formulated as nano-tauro. No detectable AZT amounts were measured in the rat CSF within 150 min after the nasal administration of both the nano-tauro suspensions.

4. Discussion

We have previously demonstrated that the ester conjugation of AZT with UDCA allows to obtain a prodrug (U-AZT) eluding the AET and improving the drug uptake by macrophages [16,17]. In particular, we obtained the permeability coefficients values (P_E) of AZT and U-AZT across monolayers constituted by retinal pigment epithelium (HRPE) cells that we used as an *in vitro* model for transport studies. The AZT P_E values from apical to basolateral compartments and *viceversa* were $209 \pm 14 \cdot 10^{-5}$ cm/min and $133 \pm 8 \cdot 10^{-5}$ cm/min ($P < 0.01$), respectively, indicating the drug involvement in active efflux processes [16]. On the other hand, the P_E values of U-AZT from apical to basolateral compartments and *viceversa* were $31.3 \pm 3.6 \cdot 10^{-5}$ cm/min and $39.1 \pm 1.2 \cdot 10^{-5}$ cm/min, respectively, indicating that the prodrug was not involved neither in active efflux nor influx processes [16]. The lower P_E values of U-AZT in comparison to those of AZT have been attributed to the high molecular weight of the prodrug (641.38 Da) that contributes to reduce its permeation across biological membranes despite its very high lipophilicity. We have then evidenced that U-AZT permeates and remains in murine macrophages with a twenty times higher efficiency than AZT [17]. Considering the lower P_E values of U-AZT with respect to those of AZT [16], the high efficiency of the prodrug to permeate in macrophages can be attributed to its ability to elude efflux phenomena.

These properties have been considered very relevant to enhance the drug anti-HIV efficacy, especially following the U-AZT delivery to the CNS. In fact, the macrophages are recognized as the only site of HIV replication in the brain [18,19]. Moving from these considerations, the aims of the present work were: (*i*) to develop innovative U-AZT formulations to further improve the prodrug macrophage uptake and (*ii*) to possibly identify a new strategy to facilitate the brain targeting of U-AZT following the administration of the developed formulations showing the highest macrophage uptake.

U-AZT is characterized by a very poor solubility in water (0.0030 ± 0.0001 mg/mL [16]), so it appeared as a good candidate to be formulated as a particulate system by nanoprecipitation, a method generally used to obtain the entrapment of lipophilic drugs in polymeric nanoparticles [33–35]. As an high homogeneity of the particle size is attributable to the excellent surfactant activity of the natural bile acid salts [36], in the present study we chose two natural bile acid salts for the formulation of U-AZT-based nanoparticles: sodium taurocholate, normally released by the gall bladder in order to emulsify hydrophobic compounds during digestion [37], and sodium ursodeoxycholate, whose acid (UDCA) is currently administered to humans against primary biliary cirrhosis [38]. The obtained nanoparticles were constituted solely by U-AZT and one of the selected bile acid salts.

We firstly observed that U-AZT allowed to obtain prodrug self-assembled cores coated by the bile acid salt corona, leading to the formation of nanoparticles with a mean diameter of ~200 nm and characterized by a very low PDI value (~0.1). Generally, PDI values smaller than 0.05 are observed in highly monodisperse standards, whereas PDI values bigger than 0.7 are related to samples with a very broad particle size distribution and probably not suitable to be analysed by the dynamic light scattering [39]. Nanoparticles obtained by self-assembling processes, like those described in this work, can have good probabilities to show PDI values near or lower than 1. This property is particularly marked in the case of taurocholate coating (nano-tauro), since nanoparticles obtained in the presence of this bile acid salt result as a perfect monodisperse system, as indicated by the extremely low PDI value (< 0.1). The role of the used bile acid salts in stabilizing the colloidal suspension of U-AZT is evidenced by the STEM images reported in Fig. 3, where dark spherical particles, attributable to the prodrug, appeared surrounded by a weak contrasted corona, attributable to the bile acid salt, whose presence may induce negative zeta potential values of the nanoparticles. In this configuration, the U-AZT content in the nanoparticles was 16.67%, according to an entrapped efficiency of 100%, as expected by the formulation procedures. The bile acid salt attribution to the coronas was confirmed by its absence following 24 h of purification of the nanoparticles by dialysis. Moreover, as illustrated in Fig. 3C, the absence of bile acid salt coating induced some aggregations of the nanoparticles, probably due to the loss of their high surface charge, related to bile acid salt properties.

The incubation of nano-tauro and nano-UDCA with the same murine macrophage preparation as used in the previous study [17] allowed us to obtain a very efficient uptake of U-AZT, which was up to seventy times higher than that displayed by U-AZT free form. These findings are in line with the aptitude of macrophages to efficiently incorporate nanoparticulate systems [20], as also confirmed by the evidence that the macrophage uptake of U-AZT free form was not significantly influenced by the presence of the selected bile acid salts.

It is worth noting that the highest U-AZT uptake values by murine macrophages were obtained with nano-tauro. Indeed, under the same incubation conditions, only 20% of nano-UDCA particles showed uptake by macrophages in comparison to the nano-tauro ones. Overall, the above results suggest that it is possible to modulate the nanoparticle macrophage uptake by choosing different bile acid salts during the nanoprecipitation procedures. This is possibly due to the influence of bile acid salt-coated nanoparticles on the activity of the macrophages, as evidenced by their different dimensional stability when suspended in complete FBS.

About the hydrolysis of the prodrug, higher AZT levels were measured in macrophages after their incubation with nanoparticulate formulations than free U-AZT. This suggests the existence of efficient nanoparticle dissolution processes within the cells, where the prodrug hydrolysis induced AZT release. The AZT concentrations detected in macrophages (Fig. 5B) were, nevertheless, sensibly lower than those of U-AZT (Fig. 5A), thus suggesting that following the nanoparticle uptake by macrophages, the dissolution process releasing the prodrug and the subsequent U-AZT hydrolysis to AZT require more than 15 min (*i.e.*, the incubation period). It must however be highlighted that the volume of the macrophages used in our experiments is 1.7 ± 0.1 pL [17], so the AZT intracellular concentrations obtained after the incubation with nano-UDCA and nano-tauro were 41.8 ± 2.4 μM and 85.9 ± 4.1 μM, respectively. It is known that AZT exhibits anti-HIV activity in HTLV-1-transformed cell line MT4, with an IC_{50} value of approximately 30 nM [40], which is more than three orders of magnitude lower than the concentration of AZT that we detected in the macrophages after incubation with the nanoparticles. As a consequence, the AZT amounts detected in macrophages following their incubation with nano-UDCA and nano-tauro appear largely sufficient to assure the anti-HIV activity of the drug.

Interestingly, no macrophage toxicity was observed during their incubation with AZT or U-AZT either in the free form or as nanoparticulate formulations.

In view of the encouraging *in vitro* results we obtained, we also performed *in vivo* experiments to possibly individuate a strategy to improve the brain targeting of the U-AZT after the administration of developed nanoparticles to rats.

It is recognized that the brain targeting of several drugs by nasal route has been studied over the last several decades [41] and, in this context, the nasal administration of nanoparticles was suggested as a potential way to address antiviral agents in the CNS [21,42,43]. In particular, the nasal administration of efavirenz (an approved antiviral drug for HIV infection) encapsulated in solid lipid nanoparticles was demonstrated to produce a ratio of drug concentration in brain to plasma about 150 times higher in comparison to that obtained by the oral administration [44]. Moreover, we have reported that with appropriate nasal formulations it is possible to drive neuroactive agents in the CSF [30,45]. The drug delivery from the nose to the CNS along the olfactory and trigeminal pathways can occur within a few minutes [46].

Based on the above findings, we hypothesized that the nasal administration of developed nanoparticulate systems may facilitate the U-AZT targeting in CNS, being unconjugated bile acid salts known as nasal absorption promoters [47]. Although bile salts can induce serious ciliary toxicity, taurocholate shows only very mild effects on nasal ciliary movement [48], thus suggesting that nano-tauro might have a better safety profile when administered *in vivo*. As nano-tauro also displayed, when compared to nano-UDCA, a higher U-AZT macrophage uptake, this formulation has been selected for the *in vivo* experiments. The zeta potential of the nano-tauro particles is negative, showing values about -60 mV. The presence of negatively charged species in the mucosal membranes can induce electrostatic repulsions and this might reduce the adhesion of nano-particles. On the contrary, chitosan, often used as nasal absorption promoter, appears characterized by good mucoadhesive properties [30] due to the positive charges of its amino groups [49]. Moreover, chitosan is known to transiently open the tight junctions of nasal mucosa, allowing to increase the CSF admittance of nasally administered drugs [22]. In line with this, it has been demonstrated the ability of chitosan to induce nanoparticles with diameters around 200 nm to cross the tight junctions of epithelial monolayers by a paracellular pathway [50]. Very recently, this phenomenon has been also evidenced on cell models of intranasal epithelium [23]. The nanotauro nasal administration was therefore performed in the absence or in the presence of chitosan.

The results demonstrate that the nasal administration of nano-tauro containing 200 μg of U-AZT allowed the rapid permeation of the prodrug in the rat CSF. The peak concentration ($\sim$3 μg/mL) was observed 60 min after the nanoparticle administration and the measured AUC value was $\sim$150 $\mu g \cdot mL^{-1} \cdot min$. Interestingly, in the presence of chitosan, a significant increase in the detected U-AZT concentrations in the rat CSF was observed. In particular, under these experimental conditions, the U-AZT peak concentration was $\sim$4 μg/mL (60 min after the administration). This value is higher than that previously obtained following the nasal administration of the same dose of U-AZT encapsulated in solid chitosan hydrochloride microparticles [17]. In the previous study, it was evidenced that the nasal administration of raw U-AZT to rats did not lead to its uptake in the rat CSF [17]. The AUC value obtained by administering nano-tauro particles in the presence of chitosan was similar to that measured following the chitosan-based U-AZT microparticle nasal administration ($\sim$300 $\mu g\, mL^{-1}$ min), thus suggesting that similar amounts of U-AZT reached the rat CSF following the nasal administration of these formulations.

Taken together, the mucoadesive properties of chitosan and its aptitude to open the mucosal tight junctions can explain the higher U-AZT concentrations in the rat CSF observed when nano-tauro were administered in the presence of this polymer.

The possibility that in the presence of chitosan the nano-tauro particles can directly reach the CSF from the nasal cavity in order to be strongly uptaken by macrophages appears intriguing. Further investigation should be necessary to elucidate these aspects.

5. Conclusions

In the present study we propose new nanoparticles constituted by a pro-drug insoluble in water (U-AZT) core coated with a bile acid salt able to modulate their uptake in macrophages. These nanoparticles, being constituted by prodrug cores coated by a bile acid salt, have been obtained by simple and cheap procedures in the absence of any other excipients, thus resulting highly biocompatible. Furthermore, we propose that depending of the coating bile acid salt, it is possible to easily obtain novel nanoparticles able to avoid or target macrophages.

After their nasal administration to rat, the most efficiently internalized nanoparticles (nano-tauro) demonstrated the ability to induce the U-AZT uptake in CSF, where macrophages constitute one of the most important and unreachable HIV sanctuaries in the body. This is particularly evident when nano-tauro were combined to chitosan. The present results can be considered an initial step toward the antiviral drug targeting of macrophages in CSF. Further investigations will be focused on the evaluation of the nano-tauro integrity in subarachnoid spaces, which is essential to exploit the relevance of this strategy in eradicating HIV settled in CSF macrophages.

From a general point of view, a low macrophage uptake, as that induced by an ursodeoxycholate corona, may be associated with a long-time circulation of the nanoparticles in the bloodstream, allowing them to reach other therapeutic sites besides macrophages; on the other hand, an efficient macrophage uptake, as that induced by a taurocholate corona, may be useful to almost specifically target a drug in macrophages. This also suggests a strategy that may be used for the nanoparticle formulation of other drugs. For example, it may be interesting to verify whether a highly lipophilic drug such as the anticancer paclitaxel can be formulated as long circulation nanoparticles coated by ursodeoxycholate, in order to avoid the use of polyethoxylated castor oil (Cremophor), a very toxic solvent normally used to solubilize the drug for human administrations [51]. Finally, the complete absence of polymers in nano-tauro and nano-UDCA particles should avoid the related toxicity and immunologic problems.

Declaration of Competing Interest

Authors declare that they have not conflicts of interest to disclose.

Acknowledgements

Support from the University of Ferrara (F72I15000470005) in the frame of the project FAR2014 is gratefully acknowledged. This work was also funded by University of Modena and Reggio Emilia (DSV-FAR 2015Leo).

References

[1] Panel on Antiretroviral Guidelines for Adults and Adolescents, Guidelines for the Use of Antiretroviral Agents in Adults and Adolescents Living with HIV, Department of Health and Human Services, National Institute of Health (NIH), USA, 2017 (accessed on April 2018).

[2] O. Lambotte, K. Deiva, M. Tardieu, HIV-1 persistence, viral reservoir and the central nervous system in the HAART era, Brain. Pathol. 13 (2003) 95–103, https://doi.org/10.1111/j.1750-3639 2003.tb00010.x.

[3] S. Aquaro, V. Svicher, D. Schols, M. Pollicita, A. Antinori, J. Balzarini, C.F. Perno, Mechanisms underlying activity of antiretroviral drugs in HIV-1-infected macrophages: new therapeutic strategies, J. Leukoc. Biol. 80 (2006) 1103–1110, https://doi.org/10.1189/jlb.0606376.

[4] P.H. Cunningham, D.G. Smith, C. Satchell, D.A. Cooper, B. Brew, Evidence for independent development of resistance to HIV-1 reverse transcriptase inhibitors in the cerebrospinal fluid, AIDS 14 (2000) 1949–1954, https://doi.org/10.1097/

00002030-200009080-00010.
[5] F. Gray, F. Scaravilli, I. Everall, F. Chretien, S. An, D. Boche, H. Adle-Biassette, L. Wingertsmann, M. Durigon, B. Hurtrel, F. Chiodi, J. Bell, P. Lantos, Neuropathology of early HIV-1 infection, Brain Pathol. 6 (1996) 1–15.
[6] P.M. Chaudhary, E.B. Mechetner, I.B. Roninson, Expression and activity of the multidrug resistance P-glycoprotein in human peripheral blood lymphocytes, Blood 80 (1992) 2735–2739.
[7] A.A. Neyfakh, A.S. Serpinskaya, A.V. Chervonsky, S.G. Apasov, A.R. Kazarov, Multidrug-resistance phenotype of a subpopulation of T-lymphocytes without drug selection, Exp. Cell Res. 185 (1989) 496–505, https://doi.org/10.1016/0014-4827(89)90318-2.
[8] O. Janneh, E. Jones, B. Chandler, A. Owen, S.H. Khoo, Inhibition of P-glycoprotein and multidrug resistance-associated proteins modulates the intracellular concentration of lopinavir in cultured CD4 T cells and primary human lymphocytes, J. Antimicrob. Chemother. 60 (2007) 987–993, https://doi.org/10.1093/jac/dkm353.
[9] S. Jorajuria, N. Dereuddre-Bosquet, F. Becher, S. Martin, F. Porcheray, A. Garrigues, A. Mabondzo, H. Benech, J. Grassi, S. Orlowski, D. Dormont, P. Clayette, ATP binding cassette multidrug transporters limit the anti-HIV activity of zidovudine and indinavir in infected human macrophages, Antivir. Ther. 9 (2004) 519–528.
[10] H.A. Namanja, D. Emmert, D.A. Davis, C. Campos, D.S. Miller, C.A. Hrycyna, J. Chmielewski, Toward eradicating HIV reservoirs in the brain: inhibiting P-glycoprotein at the blood-brain barrier with prodrug abacavir dimers, J. Am. Chem. Soc. 134 (2012) 2976–2980, https://doi.org/10.1021/ja206867t.
[11] B. Pavan, A. Dalpiaz, Prodrugs and endogenous transporters: are they suitable tools for drug targeting into the central nervous system? Curr. Pharm. Des. 17 (2011) 3560–3576, https://doi.org/10.2174/138161211798194486.
[12] B. Pavan, G. Paganetto, D. Rossi, A. Dalpiaz, Multidrug resistance in cancer or inefficacy of neuroactive agents: innovative strategies to inhibit or circumvent the active efflux transporters selectively, Drug Discov. Today 19 (2014) 1563–1571, https://doi.org/10.1016/j.drudis.2014.06.004.
[13] M.B. Lucia, R. Cauda, A.L. Landay, W. Malorni, G. Donelli, L. Ortona, Transmembrane P-glycoprotein (P-gp/P-170) in HIV infection: analysis of lymphocyte expression and drug-unrelated function, AIDS Res. Hum. Retrovir. 11 (1995) 893–901, https://doi.org/10.1089/aid.1995.11.893.
[14] N. Giri, N. Shaik, G. Pan, T. Terasaki, C. Mukai, S. Kitagaki, N. Miyakoshi, W.F. Elmquist, Investigation of the role of breast cancer resistance protein (Bcrp/Abcg2) on pharmacokinetics and central nervous system penetration of abacavir and zidovudine in the mouse, Drug Metab. Dispos. 36 (2008) 1476–1484, https://doi.org/10.1124/dmd.108.020974.
[15] N. Strazielle, M.F. Belin, J.F. Ghersi-Egea, Choroid plexus controls brain availability of anti-HIV nucleoside analogs via pharmacologically inhibitable organic anion transporters, AIDS 17 (2003) 1473–1485, https://doi.org/10.1097/00002030-200307040-00008.
[16] A. Dalpiaz, G. Paganetto, B. Pavan, M. Fogagnolo, A. Medici, S. Beggiato, D. Perrone, Zidovudine and ursodeoxycholic acid conjugation: design of a new prodrug potentially able to bypass the active efflux transport systems of the central nervous system, Mol. Pharm. 9 (2012) 957–968, https://doi.org/10.1021/mp200565g.
[17] A. Dalpiaz, M. Fogagnolo, L. Ferraro, A. Capuzzo, B. Pavan, G. Rassu, A. Salis, P. Giunchedi, E. Gavini, Nasal chitosan microparticles target a zidovudine prodrug to brain HIV sanctuaries, Antiviral Res. 123 (2015) 146–157, https://doi.org/10.1016/j.antiviral.2015.09.013.
[18] A.L. Cunningham, H. Naif, N. Saksena, G. Lynch, J. Chang, S. Li, R. Jozwiak, M. Alali, B. Wang, W. Fear, A. Sloane, L. Pemberton, B. Brew, HIV infection of macrophages and pathogenesis of AIDS dementia complex: interaction of the host cell and viral genotype, J. Leukocyte Biol. 62 (1997) 117–125.
[19] J.F. Ghersi-Egea, W. Finnegan, J.L. Chen, J.D. Fenstermacher, Rapid distribution of intraventricularly administered sucrose into cerebrospinal fluid cisterns via subarachnoid velae in rat, Neuroscience 75 (1996) 1271–1288.
[20] S. Gorantla, H. Dou, M. Boska, C.J. Destache, J. Nelson, L. Poluektova, B.E. Rabinow, H.E. Gendelman, R.L. Mosley, Quantitative magnetic resonance and SPECT imaging for macrophage tissue migration and nanoformulated drug delivery, J Leukoc. Biol. 80 (2006) 1165–1174, https://doi.org/10.1189/jlb.0206110.
[21] K.P. Seremeta, D.A. Chiappetta, A. Sosnik, Poly(ε-caprolactone), Eudragit® RS 100 and poly(ε-caprolactone)/Eudragit® RS 100 blend submicron particles for the sustained release of the antiretroviral efavirenz, Colloids Surf. B Biointerf. 102 (2013) 441–449, https://doi.org/10.1016/j.colsurfb.2012.06.038.
[22] L. Casettari, L. Illum, Chitosan in nasal delivery systems for therapeutic drugs, J. Control. Release 190 (2014) 189–200, https://doi.org/10.1016/j.jconrel.2014.05.003.
[23] I. Schlachet, A. Sosnik, Mixed mucoadhesive amphiphilic polymeric nanoparticles cross a model of nasal septum epithelium in vitro, ACS Appl. Mater. Interf. 11 (2019) 21360–21371, https://doi.org/10.1021/acsami.9b04766.
[24] H. Fessi, F. Puisieux, J.P. Devissaguet, N. Ammoury, S. Benita, Nanocapsule formation by interfacial polymer deposition following solvent displacement, Int. J. Pharm. 55 (1989) R1–R4, https://doi.org/10.1016/0378-5173(89)90281-0.
[25] F. Sacchetti, G. Marverti, D. D'Arca, L. Severi, E. Maretti, V. Iannuccelli, S. Pacifico, G. Ponterini, M.P. Costi, E. Leo, pH-promoted release of a novel anti-tumour peptide by "stealth" liposomes: effect of nanocarriers on the drug activity in cis-platinum resistant cancer cells, Pharm. Res. 35 (2018) 206, https://doi.org/10.1007/s11095-018-2489-z.
[26] K. Felgenhauer, Protein size and CSF composition, Klin. Wochenschr. 52 (1974) 1158–1164.
[27] A. Madu, C. Cioffe, U. Mian, M. Burroughs, E. Tuomanen, M. Mayers, E. Schwartz, M. Miller, Pharmacokinetics of fluconazole in cerebrospinal fluid and serum of rabbits: validation of an animal model used to measure drug concentrations in cerebrospinal fluid, Antimicrob. Agents Chemother. 38 (1994) 2111–2115, https://doi.org/10.1128/AAC.38.9.2111.
[28] S. Manfredini, B. Pavan, S. Vertuani, M. Scaglianti, D. Compagnone, C. Biondi, A. Scatturin, S. Tanganelli, L. Ferraro, P. Prasad, A. Dalpiaz, Design, Synthesis and activity of ascorbic acid prodrugs of nipecotic, kinurenic and diclophenamic acids, liable to increase neurotropic activity, J. Med. Chem. 45 (2002) 559–562, https://doi.org/10.1021/jm015556r.
[29] A. Dalpiaz, B. Pavan, S. Vertuani, F. Vitali, M. Scaglianti, F. Bortolotti, C. Biondi, A. Scatturin, S. Tanganelli, L. Ferraro, G. Marzola, P. Prasad, S. Manfredini, Ascorbic and 6-Br-ascorbic acid conjugates as a tool to increase the therapurtic effects of potentially central active drugs, Eur. J. Pharm. Sci. 24 (2005) 259–269, https://doi.org/10.1016/j.ejps.2004.10.014.
[30] A. Dalpiaz, E. Gavini, G. Colombo, P. Russo, F. Bortolotti, L. Ferraro, S. Tanganelli, A. Scatturin, E. Menegatti, P. Giunchedi, Brain uptake of an antiischemic agent by nasal administration of microparticles, J. Pharm. Sci. 97 (2008) 4889–4903, https://doi.org/10.1002/jps.21335.
[31] M.P. Van den Berg, S.G. Romeijn, J.C. Verhoef, F.W. Merkus, Serial cerebrospinal fluid sampling in a rat model to study drug uptake from the nasal cavity, J. Neurosci. Methods 116 (2002) 99–107, https://doi.org/10.1016/S0165-0270(02)00033-X.
[32] A. Dalpiaz, L. Ferraro, D. Perrone, E. Leo, V. Iannuccelli, B. Pavan, G. Paganetto, S. Beggiato, S. Scalia, Brain uptake of a zidovudine prodrug after nasal administration of solid lipid microparticles, Mol. Pharm. 11 (2014) 1550–1561, https://doi.org/10.1021/mp400735c.
[33] A. Minost, J. Delaveau, M.A. Bolzinger, H. Fessi, A. Elaissari, Nanoparticles via nanoprecipitation process, Recent Pat. Drug Deliv. Formul. 6 (2012) 250–258, https://doi.org/10.2174/187221112802652615.
[34] U. Bilati, E. Allemann, E. Doelker, Development of a nanoprecipitation method intended for the entrapment of hydrophilic drugs into nanoparticles, Eur. J. Pharm. Sci. 24 (2005) 67–75, https://doi.org/10.1016/j.ejps.2004.09.011.
[35] P.A. Grabnar, J. Kristl, The manufacturing techniques of drug-loaded polymeric nanoparticles from preformed polymers, J. Microencapsul. 28 (2011) 323–335, https://doi.org/10.3109/02652048.2011.569763.
[36] C. Faustino, C. Serafim, P. Rijo, C.P. Reis, Bile acids and bile acid derivatives: use in drug delivery systems and as therapeutic agents, Expert. Opin. Drug. Deliv. 13 (2016) 1133–1148, https://doi.org/10.1080/17425247.2016.1178233.
[37] E. Acosta, Bioavailability of nanoparticles in nutrient and nutraceutical delivery, Curr. Opin. Colloid Interf. Sci. 14 (2009) 3–15, https://doi.org/10.1016/j.cocis.2008.01.002.
[38] A. Floreani, I. Franceschet, L. Perini, N. Cazzagon, M.E. Gershwin, C.L. Bowlus, New therapies for primary biliary cirrhosis, Clin. Rev. Allergy Immunol. 48 (2015) 263–272, https://doi.org/10.1007/s12016-014-8456-5.
[39] M. Danaei, M. Dehghankhold, S. Ataei, F. Hasanzadeh Davarani, R. Javanmard, A. Dokhani, S. Khorasani, M.R. Mozafari, Impact of particle size and polydispersity index on the clinical applications of lipidic nanocarrier systems, Pharmaceutics 10 (2) (2018) 57, https://doi.org/10.3390/pharmaceutics10020057.
[40] M. Magnani, A. Casabianca, A. Fraternale, G. Brandi, S. Gessani, R. Williams, M. Giovine, G. Damonte, A. De Flora, U. Benatt, Synthesis and targeted delivery of an azidothymidine homodinucleotide conferring protection to macrophages against retroviral infection, Proc. Natl. Acad. Sci. USA 93 (1996) 4403–4408, https://doi.org/10.1073/pnas.93.9.4403.
[41] A.R. Khan, M. Liu, M.W. Khan, G. Zhai, Progress in brain targeting drug delivery system by nasal route, J. Control. Release 268 (2017) 364–389, https://doi.org/10.1016/j.jconrel.2017.09.001.
[42] A. Dalpiaz, B. Pavan, Nose-to-brain delivery of antiviral drugs: a way to overcome their active efflux? Pharmaceutics 10 (2018) 39, https://doi.org/10.3390/pharmaceutics10020039.
[43] H. Gao, Progress and perspectives on targeting nanoparticles for brain drug delivery, Acta Pharm. Sin. B 6 (2016) 268–286, https://doi.org/10.1016/j.apsb.2016.05.013.
[44] S. Gupta, R. Kesarla, N. Chotai, A. Misra, A. Omri, Systematic approach for the formulation and optimization of solid lipid nanoparticles of efavirenz by high pressure homogenization using design of experiments for brain targeting and enhanced bioavailability, Biomed. Res. Int. 2017 (2017) 5984014, https://doi.org/10.1155/2017/5984014.
[45] G. Rassu, E. Soddu, M. Cossu, A. Brundu, G. Cerri, N. Marchetti, L. Ferraro, R.F. Regan, P. Giunchedi, E. Gavini, A. Dalpiaz, Solid microparticles based on chitosan or methyl-β-cyclodextrin: a first formulative approach to increase the nose-to-brain transport of deferoxamine mesylate, J. Control. Release 10 (2015) 68–77, https://doi.org/10.1016/j.jconrel.2015.01.025.
[46] L.R. Hanson, W.H. Frey 2nd, Strategies for intranasal delivery of therapeutics for the prevention and treatment of neuroAIDS, J. Neuroimmune Pharmacol. 2 (2007) 81–86, https://doi.org/10.1007/s11481-006-9039-x.
[47] N. Pavlović, S. Goločorbin-Kon, M. Danić, B. Stanimirov, H. Al-Salami, K. Stankov, M. Mikov, Bile acids and their derivatives as potential modifiers of drug release and pharmacokinetic profiles, Front. Pharmacol. 9 (2018) 1283, https://doi.org/10.3389/fphar.2018.01283.
[48] W.A. Hermens, P.M. Hooymans, J.C. Verhoef, F.W. Merkus, Effects of absorption enhancers on human nasal tissue ciliary movement in vitro, Pharm Res. 7 (1990) 144–166.
[49] C.M. Lehr, J.A. Bouwstra, E.H. Schacht, H.E. Junginger, In vitro evaluation of mucoadhesive properties of chitosan and some other natural polymers, Int. J. Pharm. 78 (1992) 43–48, https://doi.org/10.1016/0378-5173(92)90353-4.
[50] I. Schlachet, A. Sosnik, Protoporphyrin IX-modified chitosan-g-oligo(NiPAAm) polymeric micelles: from physical stabilization to permeability characterization in

vitro, Biomater. Sci. 5 (2016) 128–140, https://doi.org/10.1039/c6bm00667a.

[51] B. Damascelli, G. Cantù, F. Mattavelli, P. Tamplenizza, P. Bidoli, E. Leo, F. Dosio, A.M. Cerrotta, G. Di Tolla, L.F. Frigerio, F. Garbagnati, R. Lanocita, A. Marchianò, G. Patelli, C. Spreafico, V. Tichà, V. Vespro, F. Zunino, Intraarterial chemotherapy with polyoxyethylated castor oil free paclitaxel, incorporated in albumin nanoparticles (ABI-007): Phase I study of patients with squamous cell carcinoma of the head and neck and anal canal: preliminary evidence of clinical activity, Cancer 92 (2001) 2592–2602, https://doi.org/10.1002/1097-0142(20011115)92:10<2592::aid-cncr1612>3.0.co;2-4.